Supplement of Biogeosciences, 23, 1459–1475, 2026
https://doi.org/10.5194/bg-23-1459-2026-supplement

Biogeosciences Open Access EGU

Supplement of

Enhanced methane cycling across the Laptev Sea signaled by time-integrated biomarkers of aerobic methane oxidation

Albin Eriksson et al.

Correspondence to: Albin Eriksson (albin.eriksson@aces.su.se) and Örjan Gustafsson (orjan.gustafsson@aces.su.se)

Abstract. Elevated methane concentrations in seawater have been reported over extensive areas of the East Siberian Arctic Seas, overlying thawing subsea permafrost. However, observed methane concentrations of the ephemeral seawater are highly variable across both space and time, compromised by both the timing of rare measurements and storm-driven exchanges to the atmosphere. Here, we applied time-integrated signals of the δ^{13}C-composition of specific C_{30} hopanoids (diploptene, hop-17(21)-ene, neohop-13(18)-ene and diplopterol) in surface sediments to trace aerobic methane oxidation as a proxy for enhanced methane cycling. Interpretations of hopanoids and possible sources were further assessed by 16S-rRNA analyses in the surface sediments. The consistently low δ^{13}C-C_{30} hopenes signals, ranging between -57.5 to -37.1 ‰ (n=23) across the Laptev Sea shelf indicated aerobic methane oxidation. This suggests ubiquitous methane cycling with the most pronounced intensities in the outer shelf region, broadly consistent with the observed methane concentrations. Notably, depleted δ^{13}C-C_{30} hopenes were also found in the mid-shelf region of the Laptev Sea, earlier thought to be an area of comparatively low methane cycling. High methane concentrations were also observed in the vicinity of the Lena River delta, yet the isotopically heavier δ^{13}C-C_{30} hopenes may here reflect a combination of lower aerobic methane oxidation, a greater relative abundance of type II methanotrophs (lower isotope fractionation during hopanoid production) and isotope dilution from non-methanotrophic sources. While this complicates the biomarker interpretation in the unique setting near the Lena River delta, the δ^{13}C-C_{30} hopenes were still much lower than δ^{13}C-organic carbon, indicating aerobic methane oxidation and a clear methane cycling signal also in this regime. Taken together, the results unravel the wider cross-shelf patterns of enhanced methane cycling in the Laptev Sea through probing of methane fossilised in membrane lipids of aerobic methanotrophs, with the molecular-isotopic pattern being preserved in the sedimentary archive.

Table of contents

1 Supplementary results and figures

The investigated Laptev Sea sediments contained a variety of non-methanotrophic hopanoid producers, including heterotrophs and autotrophs. Particularly, the sum of non-methanotrophic hopanoid producers displayed the highest relative abundance in the ILS (mean±standard deviation= 0.60±0.48 %, n=3). Non-methanotrophic hopanoid producers were a mix of *Burkholderia*, *Acidobacteria*, and *Cyanobacteria* (Fig. S2). On the contrary, in the MLS/OLS, the relative abundance of non-methanotrophic hopanoid producers was very low (0.04±0.03 %, n=2; 0.02±0.01 %, n=4). Taken together, MOB-I constituted the largest part of the bacterial hopanoid producers in the OLS, whereas hopanoid producers in the ILS/MLS were a mix of MOB-I/II and non-methanotrophic hopanoid producers, primarily heterotrophic bacteria (Fig.4).

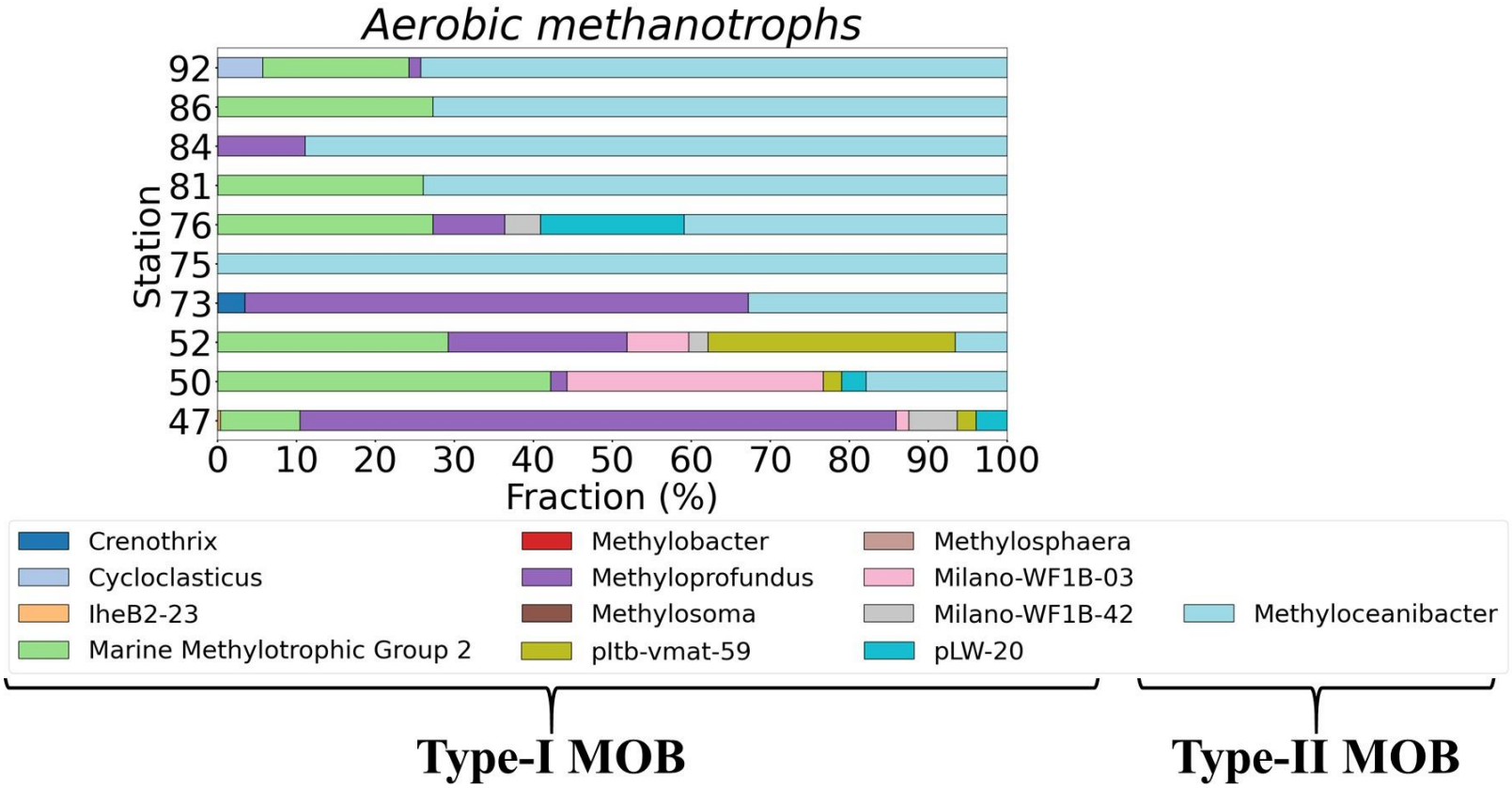

Figure S1: Percentual composition of aerobic methanotrophs based on 16S-rRNA sequencing from surface sediments. Methane Oxidizing Bacteria (MOB) utilizing the ribulose monophosphate pathway (Type I MOB) and the serine pathway (Type II MOB) for formaldehyde fixation.

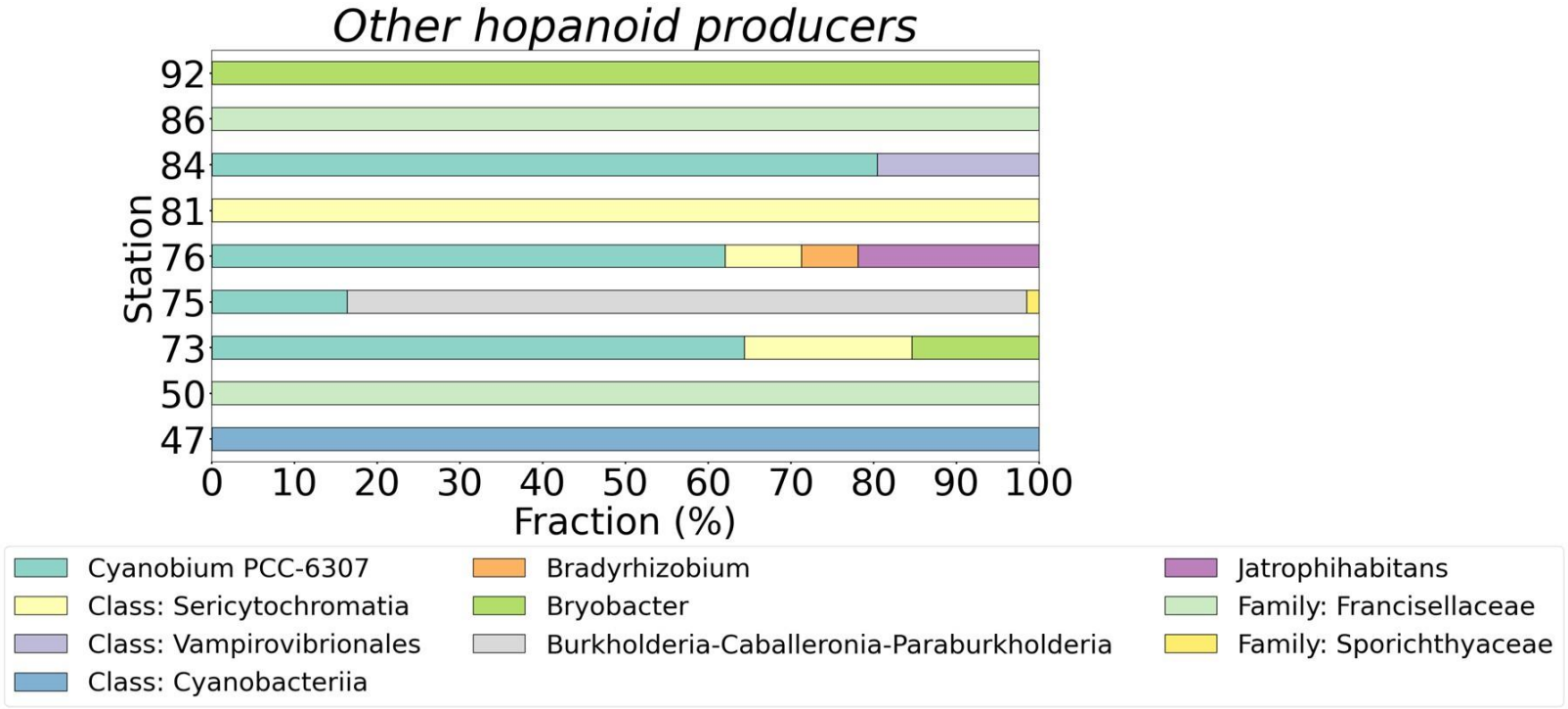

Figure S2: Percentual composition of non-methanotrophic hopanoid producers in surface sediments based on 16S-rRNA sequencing.

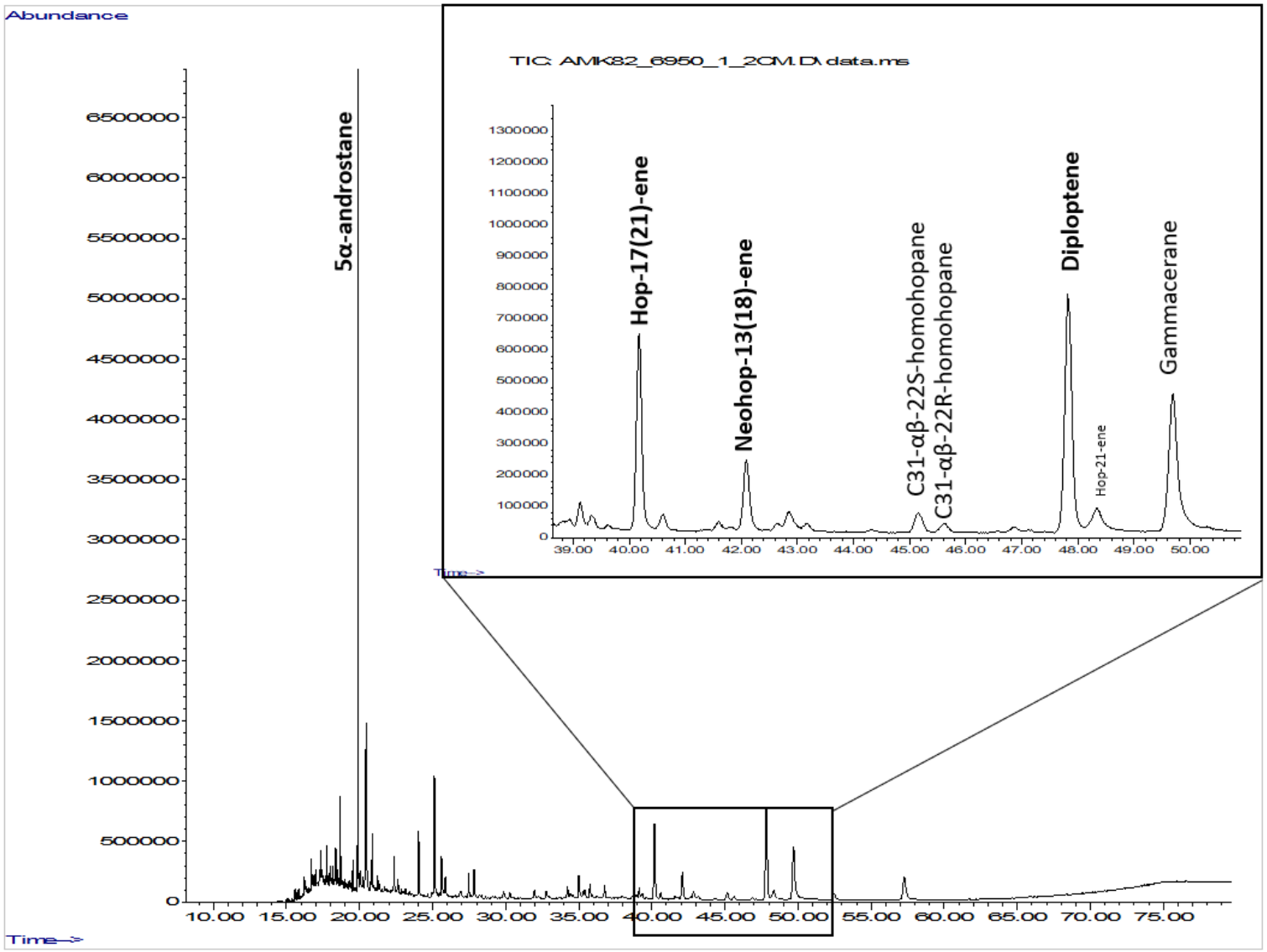

Figure S3. Total ion chromatogram (TIC) of the non-polar cyclic/branched hydrocarbon fraction, analyzed with GC-MS.

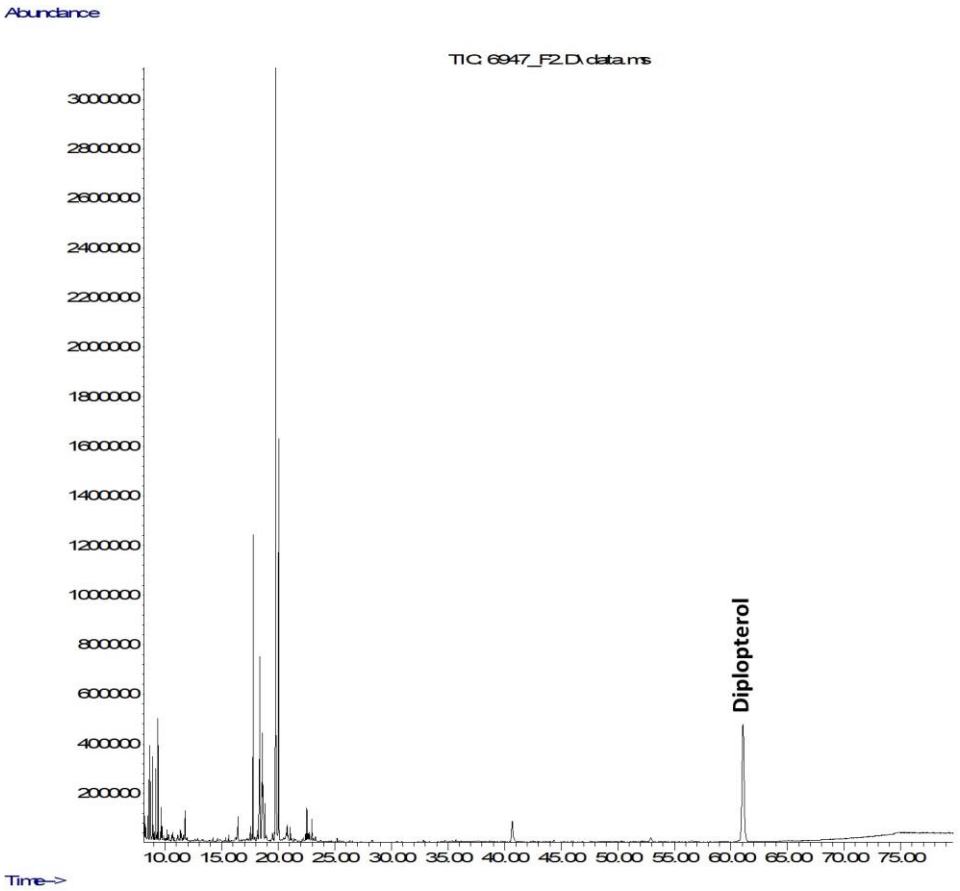

Figure S4. Total ion chromatogram (TIC) of the silylated diplopterol fraction, analyzed with GC-MS.

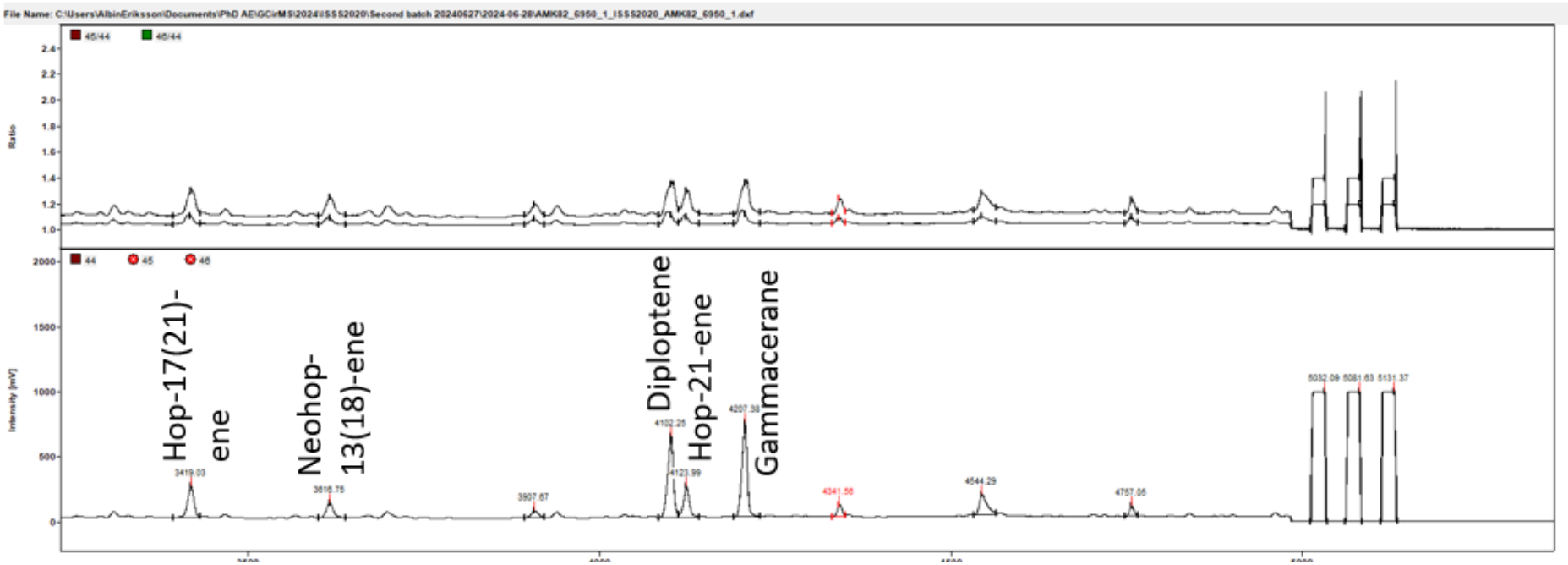

Figure S5. Partial chromatogram of mass 44, and isotope ratios (45/44 & 46/44) of the non-polar cyclic/branched hydrocarbon fraction in GC-irMS.

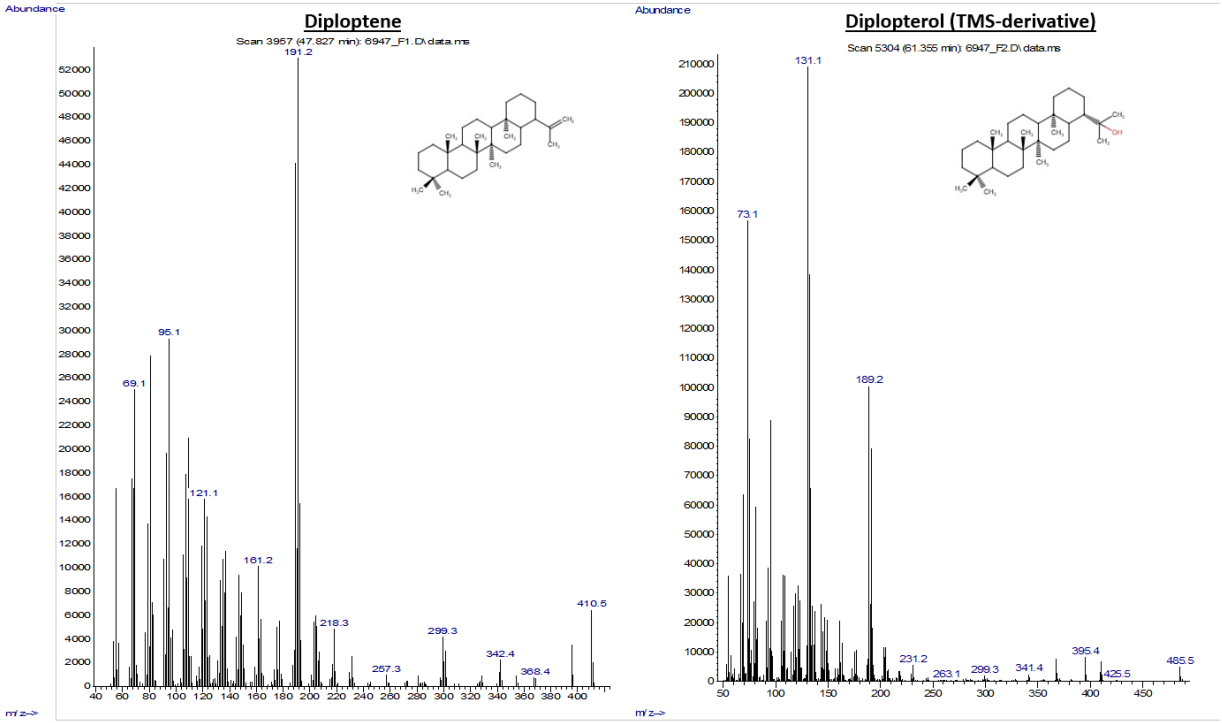

Figure S6. Electron ionization mass spectrums of diploptene and the trimethylsilyl (TMS)-derivative of diplopterol.

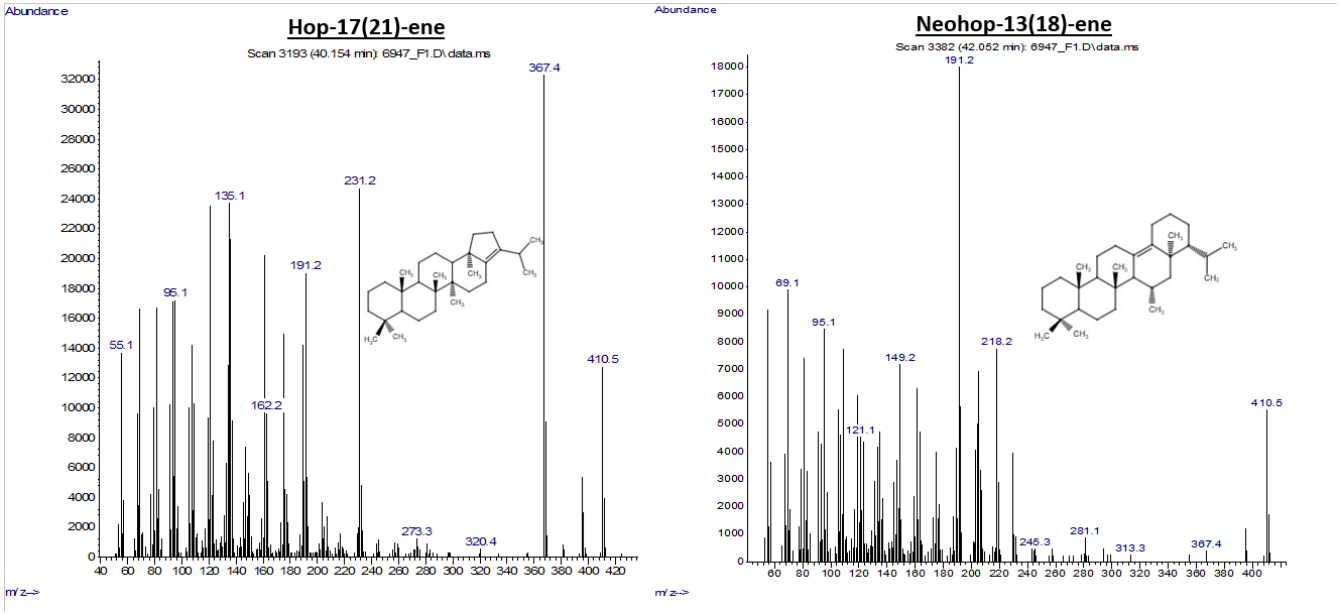

Figure S7. Electron ionization mass spectrums of hop-17(21)-ene and neohop-13(18)-ene.

2 Supplementary tables

Table S1. Statistical comparisons of sub pycnocline water CH_4 concentrations in the Outer Laptev Sea hotspot region (OLS), Mid-outer Laptev Sea transect (OLS), and the Inner Laptev Sea hotspot region (ILS).

Sub-pycnocline CH_4 concentrations in different regions (OLS, MLS, ILS)			
One-way Welch's ANOVA			
F= 53.577	num df = 2	denom df = 77.928	p-value = 2.303 e-15
Games-Howell test			
Region	p-value adjusted		
ILS vs. MLS	1.39 e-11	n = 56 vs. 16	
ILS vs. OLS	4.0 e-3	n = 56 vs. 62	
MLS vs. OLS	5.03 e-6	n = 16 vs. 62	

Table S2. Statistical comparisons of surface water versus sub-pycnocline CH_4 concentrations in the Outer Laptev Sea hotspot region (OLS), Mid-outer Laptev Sea transect (OLS), and the Inner Laptev Sea hotspot region (ILS).

t-Test: Two-Sample Assuming Unequal Variances

	OLS		MLS		ILS	
	Sub-pycnocline CH4 (nM)	*Surface water CH4 (nM)*	*Sub-pycnocline CH4 (nM)*	*Surface water CH4 (nM)*	*Sub-pycnocline CH4 (nM)*	*Surface water CH4 (nM)*
Mean	1199.7	34.1	27.0	16.9	439.7	97.0
Variance	3036093.0	756.7	327.6	18.1	117790.5	2196.8
Observations	62.0	10.0	16.0	5.0	56.0	6.0
Hypothesized Mean Difference	0.0		0.0		0.0	
df	61.0		19.0		57.0	
t Stat	5.3		2.1		6.9	
P(T<=t) one-tail	9.7E-07		2.7E-02		2.4E-09	
t Critical one-tail	1.7		1.7		1.7	
P(T<=t) two-tail	1.9E-06		5.4E-02		4.7E-09	
t Critical two-tail	2.0		2.1		2.0	

Table S3. Statistical comparisons of surface water CH_4 concentrations in the Outer Laptev Sea hotspot region (OLS), Mid-outer Laptev Sea transect (OLS), and the Inner Laptev Sea hotspot region (ILS).

Surface water CH_4 in different regions (OLS, MLS, ILS)			
One-way Welch's ANOVA			
F= 9.6358	num df = 2	denom df = 8.9395	p-value = 0.005876
Games-Howell test			
Region	p-value adjusted		
ILS vs. MLS	0.019	n = 6 vs. 5	
ILS vs. OLS	0.046	n = 6 vs. 10	
MLS vs. OLS	0.183	n = 5 vs. 10	

Table S4: Statistical comparisons of C_{30}-hopene (diploptene, hop-17(21)-ene, and neohop-13(18)-ene) concentrations in the Outer Laptev Sea hotspot region (OLS), Mid-outer Laptev Sea transect (OLS), and the Inner Laptev Sea hotspot region (ILS).

C_{30}-hopenes (µg/gOC) in different regions (OLS, MLS, ILS)			
One-way Welch's ANOVA			
F= 9.4527	num df = 2	denom df = 12.004	p-value = 0.003424
Games-Howell test			
Region	p-value adjusted		
ILS vs. MLS	0.302	n = 6 vs. 4	
ILS vs. OLS	0.064	n = 6 vs. 15	
MLS vs. OLS	0.001	n = 4 vs. 15	

Table S5: Statistical comparisons of $\delta^{13}C_{30}$-hopene (diploptene, hop-17(21)-ene, and neohop-13(18)-ene) concentrations in the Outer Laptev Sea hotspot region (OLS), Mid-outer Laptev Sea transect (OLS), and the Inner Laptev Sea hotspot region (ILS).

$\delta^{13}C$-C_{30}-hopenes in different regions (OLS, MLS, ILS)			
One-way Welch's ANOVA			
F= 43.871	num df = 2	denom df = 8.9982	p-value = 2.288e-5
Games-Howell test			
Region	p-value adjusted		
ILS vs. MLS	0.058	n = 5 vs. 4	
ILS vs. OLS	0.000000223	n = 5 vs. 15	
MLS vs. OLS	0.0000803	n = 4 vs. 15	

3 Bayesian stable isotope mixing model

A Bayesian stable isotope mixing model was applied to calculate the hopanoid source contribution. The contribution of Methane Oxidizing Bacteria (MOB)-I and II were weighted against the relative fraction of MOB in each region (Eq.2). The weighted $\delta^{13}C_{MOB}$ endmembers in each region, as well as the $\delta^{13}C$ of carbon sources and associated isotope fractionation are displayed in Tables S6 and S7. The endmember values of the CH_4 sources were calculated as the average of sub pycnocline measurements between the 2.5th and 97.5th percentile. The stable isotope mixing model was applied using "simmr" (Parnell et al., 2013), and two sources for each region, the weighted $\delta^{13}C$-MOB and $\delta^{13}C$-DOC.

Table S6: Endmembers used to calculate the percentual contribution of different carbon sources to hopanoid production.

Region	Endmember	$\delta^{13}C$-endmember (‰)	$\delta^{13}C$-endmember (standard deviation, ‰)	Endmember source
OLS	CH_4	-45,35	8,24	Steinbach et al., 2021
ILS	CH_4	-67,11	6,51	Brussee et al., 2026
MLS	CH_4	-46,51	4,78	Brussee et al., 2026
OLS	DOC	-26,81	0,84	Salvado et al., 2016
MLS	DOC	-26,81	0,84	Salvado et al., 2016
ILS	DOC	-26,81	0,84	Salvado et al., 2016
OLS	MOB	-69,71	8,51	Eq.2
MLS	MOB	-52,97	2,53	Eq.2
ILS	MOB	-82,92	8,36	Eq.2

Table S7: Isotope fractionation associated with hopanoid biosynthesis, used in the Bayesian isotope mixing model, and to establish the $\delta^{13}C_{MOB}$ endmembers.

Compound	$\Delta\delta^{13}$C-substrate-hopanoid (‰)	Standard deviation (‰)	Bacterial source	Source
MOB-I	-30,30	3,24	*Methylomonas methanica*	Jahnke et al., 1999
MOB-II	-1,01	8,77	*Methylosinus trichosporium*	Jahnke et al., 1999
Heterotrophs	-7,90	4,25	*Frankia soli* & *K. xylunis*	Schwartz et al., 2023

4 Supplementary references

Brussee, M., Holmstrand, H., Wild, B., Kosmach, D., Chernykh, D., Shakhova, N., Kurilenko, A., Semiletov, I., and Gustafsson, Ö.: Triple-isotopic analyses pinpoint microbial methane release from subsea permafrost in the inner Laptev Sea, Commun Earth Environ, https://doi.org/10.1038/s43247-026-03222-7, 2026.

Jahnke, L. L., Summons, R. E., Hope, J. M., and Des Marais, D. J.: Carbon isotopic fractionation in lipids from methanotrophic bacteria II: The effects of physiology and environmental parameters on the biosynthesis and isotopic signatures of biomarkers, Geochim. Coscmochim. Acta, 63, 79–93, https://doi.org/10.1016/S0016-7037(98)00270-1, 1999.

Parnell, A. C., Phillips, D. L., Bearhop, S., Semmens, B. X., Ward, E. J., Moore, J. W., Jackson, A. L., Grey, J., Kelly, D. J., and Inger, R.: Bayesian stable isotope mixing models, Environmetrics, 24, 387–399, https://doi.org/10.1002/env.2221, 2013.

Salvadó, J. A., Tesi, T., Sundbom, M., Karlsson, E., Krusä, M., Semiletov, I. P., Panova, E., and Gustafsson, Ö.: Contrasting composition of terrigenous organic matter in the dissolved, particulate and sedimentary organic carbon pools on the outer East Siberian Arctic Shelf, Biogeosciences, 13, 6121–6138, https://doi.org/10.5194/bg-13-6121-2016, 2016.

Schwartz-Narbonne, R., Schaeffer, P., Lengger, S. K., Blewett, J., Martin Jones, D., Motsch, E., Crombie, A., Jetten, M. S. M., Mikkelsen, D., Normand, P., Nuijten, G. H. L., Pancost, R. D., and Rush, D.: Bacterial physiology highlighted by the δ13C fractionation of bacteriohopanetetrol isomers, Org Geochem, 181, https://doi.org/10.1016/j.orggeochem.2023.104617, 2023.

Steinbach, J., Holmstrand, H., Shcherbakova, K., Kosmach, D., Brüchert, V., Shakhova, N., Salyuk, A., Sapart, C. J., Chernykh, D., Noormets, R., Semiletov, I., and Gustafsson, Ö.: Source apportionment of methane escaping the subsea permafrost system in the outer Eurasian Arctic Shelf, https://doi.org/10.1073/pnas.2019672118/-/DCSupplemental, 2021.